THE JOURNAL OF PHYSICAL CHEMISTRY C

Article

Cite This: J. Phys. Chem. C 2019, 123, 14652−14661

pubs.acs.org/JPCC

The Relation between Rotational Dynamics of the Organic Cation and Phase Transitions in Hybrid Halide Perovskites

Sudeep Maheshwari,[†] Magnus B. Fridriksson,[†] Sayan Seal,[‡] Jörg Meyer,[‡] and Ferdinand C. Grozema*[,†]

[†]Department of Chemical Engineering, Delft University of Technology, P.O. Box 5045, 2629 HZ Delft, The Netherlands

[‡]Gorlaeus Laboratories, Leiden Institute of Chemistry, Leiden University, P.O. Box 9502, 2300 RA Leiden, The Netherlands

Supporting Information

ABSTRACT: The rotational dynamics of an organic cation in hybrid halide perovskites is intricately linked to the phase transitions that are known to occur in these materials; however, the exact relation is not clear. We have performed detailed model studies on methylammonium lead iodide and formamidinium lead iodide to unravel the relation between rotational dynamics and phase behavior. We show that the occurrence of the phase transitions is due to a subtle interplay between dipole−dipole interactions between the organic cations, specific (hydrogen bonding) interactions between the organic cation and the lead iodide lattice, and deformation of the lead iodide lattice in reaction to the reduced rotational motion of the organic cations. This combination of factors results in phase transitions at specific temperatures, leading to the formation of large organized domains of dipoles. The latter can have significant effects on the electronic structure of these materials.

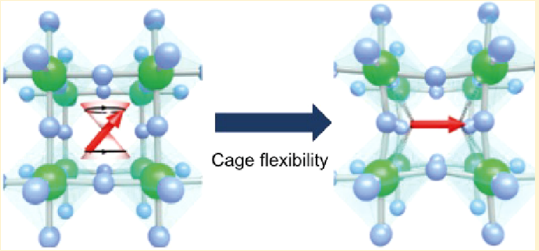

INTRODUCTION

Hybrid halide perovskites are currently among the most studied emerging solar cell materials, with reported device efficiencies well over 20% within 10 years after the first demonstration of a halide perovskite-based cell.[1−3] Hybrid halide perovskites consist of a general ABX_3 structure, where B is a doubly charged metal ion such as lead or tin and X is a halide anion. A is a singly charged cation that in the case of hybrid perovskites is an organic ammonium compound such as methylammonium (MA) or formamidinium (FA). The metal and the halide ions together form an inorganic octahedral lattice with cages that are filled by the organic cations. The most common organic cation, methylammonium, has an asymmetric charge distribution resulting in a net dipole moment. At room temperature, the dipolar MA cation can rotate almost freely inside the metal halide lattice. This leads to a high dielectric screening compared to halide perovskites with nondipolar cations such as Cs^+.[4] It has also been proposed that the dipolar nature of MA plays an important role in the optoelectronic properties of hybrid halide perovskites, for instance through the formation of ferroelectric domains that promote formation of free charges on photoexcitation or through polaronic effects that enhance the charge carrier lifetime.[5,6] The rotational freedom of MA has been found to be highly dependent on temperature, and specific phase transitions are known to occur. For instance, methylammonium lead iodide (MAPI) has a cubic structure at temperatures above 330 K, in which the MA can rotate freely. Between 170 and 330 K a tetragonal phase is formed, in which the rotational motion is somewhat restricted. At temperatures below 170 K an orthorhombic phase is present where the rotational motion is fully absent.[7] In previous experimental work we have shown that the rotational freedom of the organic cation has a direct effect on the mobility and recombination kinetics of charges in MAPI.[8] Therefore, the rotational dynamics of organic cations in hybrid perovskites has received considerable attention, both experimentally and theoretically.[9−12] However, the relation to the phase behavior and its effect on the optoelectronic properties of hybrid halide perovskites are not fully understood.

Most of the previous work has focused on the rotation of the MA ion in MAPI as this is the most investigated of the hybrid perovskites in solar cells. Experimentally, this includes solid-state NMR measurements,[9] single crystal X-ray measurements,[13] Raman spectroscopy,[13] and quasi-elastic neutron scattering.[10] Theoretically, Monte Carlo simulations have been performed[5,14] as well as density functional theory studies[15,16] and both *ab initio* molecular dynamics[17−19] and model potential molecular dynamics.[12,20,21] Most of these studies agree that at high temperatures the MA ion rotates freely without forming any ferroelectric or antiferroelectric domains, while below a certain phase transition temperature an orthorhombic phase is formed where the dipole rotation is frozen. The cause and effect relationship between the dipole dynamics and the phase transition is not fully understood. While most argue that the transfer to orthorhombic phase is

Received: March 22, 2019
Revised: May 17, 2019
Published: May 22, 2019

DOI: 10.1021/acs.jpcc.9b02736
J. Phys. Chem. C 2019, 123, 14652−14661

the source of the restricted motion of the MA ions, some have suggested that the deformation of the lead iodide cage is caused by formation of ordered domains of dipoles at low temperatures.[15]

For formamidinium lead halide perovskites (FAPI) there is a lot less information. The FA cation is larger than MA, which may restrict its rotational motion by steric interactions. It also has an almost negligible dipole moment, and it contains two nitrogen positions including hydrogens that can form hydrogen bonds with the lead iodide cage. FAPI exhibits a high-temperature cubic perovskite structure[22] and a low-temperature structure with octahedral tilting.[23] Carignano et al. have performed *ab initio* molecular dynamics simulations on FAPI and reported that at high temperatures there are preferential alignments of the FA ion due to hydrogen bonds with the cage.[24] They also concluded that FA rotates preferentially around the N−N axis, which has later been supported by other studies.[23,24] Weber et al. reported that FA shows a certain ordering at low temperature where they align perpendicular with respect to their nearest neighbor due to the angle tilt of the cage.[25]

The time scale of the reorientation of the organic cation has been studied both theoretically and experimentally for both MAPI and FAPI with varying conclusions.[26] Experimentally, methods such as neutron scattering experiments, two-dimension infrared spectroscopy, and solid-state NMR have been employed, giving time scales of reorientation for MA ranging from 1.7 to 108 ps at room temperature[5,9,11,23,26−29] and 2.8 to 8.7 ps for FA under the same conditions.[23,26,29,30] A few papers have studied both MAPI and FAPI and therefore given a direct comparison of the time scales. Fabini et al. found time scales of similar magnitude for MA and FA, 7 and 8 ps, respectively.[23] Kubicki et al., on the other hand, found FA to reorient much faster than MA, 8.7 and 108 ps, respectively.[29] Theoretically molecular dynamics simulations have also been performed to investigate the motion of the organic cation, either by *ab initio* dynamics or by using classical force fields. From such simulations a reorientation time of ∼7 ps has been obtained for MA at room temperature[17,19,21] and values of 4.3 ps[24] and 8.8 ps[25] for FA under the same conditions.

In this article we have studied the relation between the reorientation dynamics of MA and FA in MAPI and FAPI and their phase transition behavior. Apart from just performing full molecular dynamics simulations, we have also performed a series of model calculations to clarify the role of specific interactions in the system. These model calculations include on-lattice Metropolis Monte Carlo simulations to study domain formation in a system with only dipole−dipole interactions and molecular dynamics simulations with a frozen cage. Together, these calculations give a new picture of the origin of the structural phase transitions in hybrid perovskites, which shows that they are caused by an interplay between dipole−dipole interactions, specific (hydrogen bonding) interaction between the organic cation, and the inorganic cage and deformation of the metal halide cage.

METHODS

Molecular Dynamics. The molecular dynamics (MD) simulations were performed on a supercell of 10 × 10 × 10 unit cells with periodic boundary conditions for MAPI and FAPI. The system size was chosen to access better statistics and independence of motion of dipoles in different parts of the system. The initial configuration was selected as cubic for both MAPI and FAPI with a lattice constant of 6.21 Å for MAPI and 6.36 Å for FAPI as observed experimentally at higher temperatures for both of these materials.[5,22] The force field for the interatomic potentials was adopted from the work of Mattoni et al.[12] The interactions in the force field are defined in the form of three components: (i) inorganic−inorganic (U_{ii}), (ii) inorganic−organic (U_{io}), and (iii) organic−organic (U_{oo}) interactions. The U_{ii} and U_{io} are nonbonded interactions which are defined in terms of Buckhingam and Lennard-Jones parameters that take into account electrostatic and van der Waals interactions, respectively. U_{oo} interactions are defined as bonded interactions with parameters for bond stretching, angle bending, and dihedral rotations for the organic cations. We obtained these parameters from the CHARMM force field using the SwissParam tool.[31−34] MD simulations were performed using the LAMMPS molecular dynamics simulation package.[35] The equations of motion were evaluated by using time step of 1 fs and a cutoff of 17 Å for Lennard-Jones interactions and 18 Å for the Coulombic interactions. Simulations were performed in a sequence of three steps in which first step was annealing of the system with an initial configuration of ordered orientations of MA/FA molecules. The annealing was performed from a higher temperature to the temperature required for the system over 3 ns. The second step was the equilibration of the system at the required temperature until the energy of system comes to an equilibrium. The third step was the production run from which a trajectory file covering 100 ps was obtained. The rotational dynamics of the organic cations in MAPI and FAPI was analyzed by examining the rotation-autocorrelation function, $C(t)$, as defined in eq 1 in terms of the dipole vectors μ_i of the MA and FA cations. For MA this vector coincides with the C−N axis, while for FA it is along the C−H bond.

$$C(t) = \frac{1}{N}\sum_{i=1}^{N} \vec{\mu}_i(t)\cdot\vec{\mu}_i(0) \tag{1}$$

This autocorrelation function gives a measure of how fast the orientations of the organic cations change with time. By definition, $C(t = 0) = 1$ and decays to zero on average once the direction of the dipole has become completely random.

Monte Carlo. The Metropolis Monte Carlo (MC) simulations were performed on a system consisting of 20 × 20 × 20 dipoles on a fixed grid with periodic boundary conditions. A cubic structure is assumed for all temperatures with a lattice constant of 6.29 Å. The only energy considered in the simulation is the (electrostatic) dipole−dipole interaction given by eq 2. In this equation, p_i and p_j are the dipole moment vectors for both dipoles considered, r is the distance between the dipoles, and $\hat{n}$ is a unitary directional vector between the two dipoles. The permittivity of a vacuum is assumed, ignoring any dielectric screening. This will lead to some overestimation of dipole−dipole interaction compared to physical systems. Only interactions between dipoles that are within three lattice distances of one another are considered. This is a reasonable assumption since the interaction energy is inversely proportional to the third power of the distance. The simulations were performed for both MA and FA dipoles at temperatures ranging from 100 to 350 K with a 10 K interval.

$$E_{dd} = \frac{1}{4\pi\epsilon_0}\left(\frac{p_i p_j}{r^3} - \frac{3(\hat{n}\cdot p_i)(\hat{n}\cdot p_j)}{r^3}\right) \tag{2}$$

DOI: 10.1021/acs.jpcc.9b02736
J. Phys. Chem. C 2019, 123, 14652−14661

Domain Detection. The domain detection aims to quantify how ordered or disordered the organic cations are at various temperatures in the MC and MD simulations based on dipole−dipole interaction. It does so by ordering all the dipoles in a simulation snapshot on a fixed grid and choosing a random dipole in the system. This dipole is the first dipole in the first domain. Next we evaluate which, if any, of the six closest neighbors of the dipole belong in the same domain. This is done by comparing the orientations of those dipoles with the orientations that would minimize the dipole−dipole interaction energy between each of them and our first dipole. If their orientation is close enough to this minimum-energy alignment, they are added to the domain. The domain is then allowed to grow by evaluating the neighbors of the dipoles that were added to the domain. When all appropriate dipoles have been added to the domain, the process is repeated considering all the dipoles in the system that have not been assigned to a domain. Finally, when all the dipoles have been assigned to a domain, the average domain size is calculated. A large average domain size will then represent a more ordered system than a small one.

RESULTS AND DISCUSSION

Molecular dynamics and Monte Carlo simulations were performed for both MAPI and FAPI, and we have subdivided the discussion in two parts. First we discuss the dipole dynamics and phase transitions in MAPI, after which we turn to FAPI. The results in both materials are compared and some general conclusions are presented after these sections.

Methylammonium Lead Iodide (MAPI). From the molecular dynamics simulation of MAPI, a trajectory of 100 ps is obtained after equilibration of the system. The rotation-autocorrelation function over these 100 ps, averaged over the 1000 MA dipoles in the system, is shown in Figure 1a for temperatures between 100 and 350 K. The rotation-autocorrelation plots show the randomization of the direction of the dipole moments with time.

At lower temperatures (100−250 K) the autocorrelation plots show a different trend than those at higher temperature. After an initial rapid decay, an almost constant value is obtained, indicating that no full randomization of the dipole direction occurs on the time scale of the simulations. The rapid initial decay corresponds to a wobbling-like motion where the dipolar molecule can move around in a cone but does not have enough rotational freedom for complete reorientation. The more pronounced initial decay at 150 and 200 K, as compared to that at 100 K, indicates that the cone in which movement takes place widens with temperature. To quantify the time scale of dipole relaxation times, the autocorrelation curves were fitted with a biexponential function given in eq 3. A_1 and A_2 are the amplitudes of the two decay components characterized by the decay times τ_1 and τ_2. The two time constants can relate to different processes, e.g., the in-place wobbling motion and the full reorientation mentioned in the introduction. The parameters from fitting eq 3 are summarized in Table 1.

$$y = A_1 e^{-t/\tau_1} + A_2 e^{-t/\tau_2} \quad (3)$$

At temperatures of 250 K and lower, two very distinct time scales are found from the biexponential fit: a fast one that is typically on the order of 2.5 ps and a very slow one that exceeds the time scale of the simulations. The fast initial decay corresponds to the in-place wobbling of the MA dipole, while the long-time decay corresponds to the full reorientation. The long-time decay constant of 450 ps and longer for these temperature indicates that the dipole orientation is virtually fixed on the time scale considered. Above 250 K the rotation-autocorrelation curves completely decay to zero within ≈5 ps. This indicates that at this temperature range MA dipoles have full rotational freedom and behave almost liquid-like. At these temperatures the decay of the autocorrelation can be described

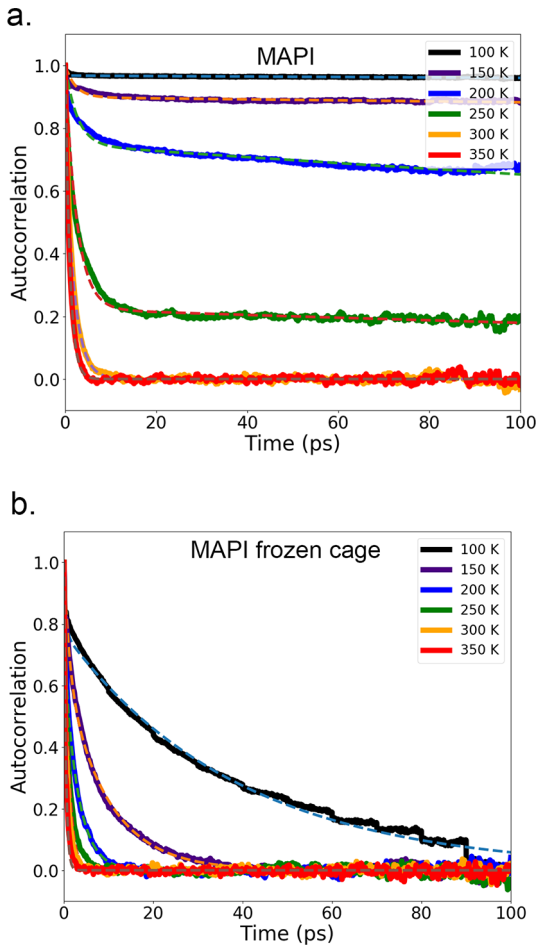

Figure 1. (a) Rotation autocorrelation of the dipole direction averaged over 1000 dipoles for MA cations in a flexible lead iodide cage at temperatures ranging from 100 to 350 K. (b) Rotation autocorrelation of the dipole direction averaged over 1000 dipoles for MA cations in a frozen lead iodide cage at temperatures ranging from 100 to 350 K.

Table 1. Rotation-Autocorrelation Decay Time Constants for MA (in picoseconds) Obtained after Fitting the Decay Curves in Figure 1 by Using Eq 3[a]

	flexible cage		frozen cage	
T (K)	τ_1 (ps) (A_1)	τ_2 (ps) (A_2)	τ_1 (ps) (A_1)	τ_2 (ps) (A_2)
100	0.12 (0.03)	>1000 (0.97)	0.42 (0.23)	38.75 (0.77)
150	2.26 (0.10)	>1000 (0.90)	1.23 (0.35)	9.54 (0.65)
200	2.62 (0.25)	739.27 (0.75)	0.27 (0.30)	3.10 (0.70)
250	2.52 (0.78)	455.57 (0.22)	1.03 (1.00)	
300	0.46 (0.25)	2.00 (0.75)	0.63 (1.00)	
350	1.01 (1.00)		0.43 (1.00)	

[a] τ_1 corresponds to the faster decay time, whereas τ_2 corresponds to the slower decay time constant.

DOI: 10.1021/acs.jpcc.9b02736
J. Phys. Chem. C 2019, 123, 14652−14661

with a single-exponential function with characteristic time constants of 0.5−2.0 ps. It is interesting to note that at these temperatures no distinction can be made between the wobbling motion and full reorientation. If the 300 K time constant is compared with previous experimental and theoretical work, the full reorientation is slightly faster than in most cases but is still of the same order of magnitude.[26] These slight difference can be caused by shortcomings of the MD force field to describe the exact temperature behavior of the structure. The observed changes in rotational dynamics with temperature agree with experimentally observed phase dynamics and with earlier molecular dynamics simulation.[9,27,36]

While the molecular dynamics simulations successfully describe the phase behavior in MAPI, at least qualitatively, the details of the relation between the dynamics of the MA cations and the phase transition are not fully clear. We have identified three possible effects that can play a role in this. The first is the deformation of the Pb−I cages. The reduced rotation of MA at low temperatures can be caused by the deformation of the cages, or the reduced dipole rotation causes the deformation itself. The second effect is the interaction between the different MA cations in the system, which can lead to ordered domains with restricted rotational dynamics at low temperature. Finally, the third effect is related to specific interactions between the MA cation and the Pb−I cage structure, for instance, hydrogen bonds between the ammonium and iodide ions. To clarify the importance of these three effects, we have performed a series of model simulations that are outlined below.

Effect of Cage Deformation. To establish the importance of the deformation of the Pb−I framework on the rotational dynamics of the MA ions, we have performed model calculations in which the positions of Pb and I are frozen in the initial cubic conformation. In this way we can obtain insight into the motion of the organic cations in the presence of specific interactions with the Pb−I cage and interactions with different organic cations, but in the absence of deformation of the cage. As evident from Figure 1b and Table 1, the rotation-autocorrelation function decreases faster than for a flexible cage. The decay time of the autocorrelation function decreases uniformly as the temperature is increased from 100 to 350 K. No sudden change is observed in the rotation time at 200 K for the frozen cage. This shows that the rotational motion of the organic cation is highly influenced by deformation of the Pb−I framework, especially at low temperatures.

Effect of Dipole−Dipole Interactions. The second specific interaction we look at is dipole−dipole interactions between the MA ions. To investigate to what extent these interactions affect the alignment of MA, we have performed MC simulations at various temperatures. In these simulations only the dipole−dipole interaction energy is taken into account. Therefore, any formation of organized domains observed is solely due to these electrostatic interactions between MA ions and not because of cage deformation or, for instance, hydrogen bonding with iodide. A convenient way to quantify the alignment of the MA dipolar ions with respect to each other is to look at snapshots of the simulations and divide all the ions into domains based on close range dipole−dipole interactions. A large domain then represents a certain long-range ordering of dipoles. In Figure 2a the average domain size in the MC simulations is plotted versus the temperature. As these systems only depend on the dipole−dipole interaction energy, lowering the temperature forces the dipoles to align more optimally with the other dipoles and especially their closest neighbors. This results in an exponential increase of average domain size as the temperature approaches 100 K, while at higher temperatures the systems is rather disordered as indicated by the smaller average domain size.

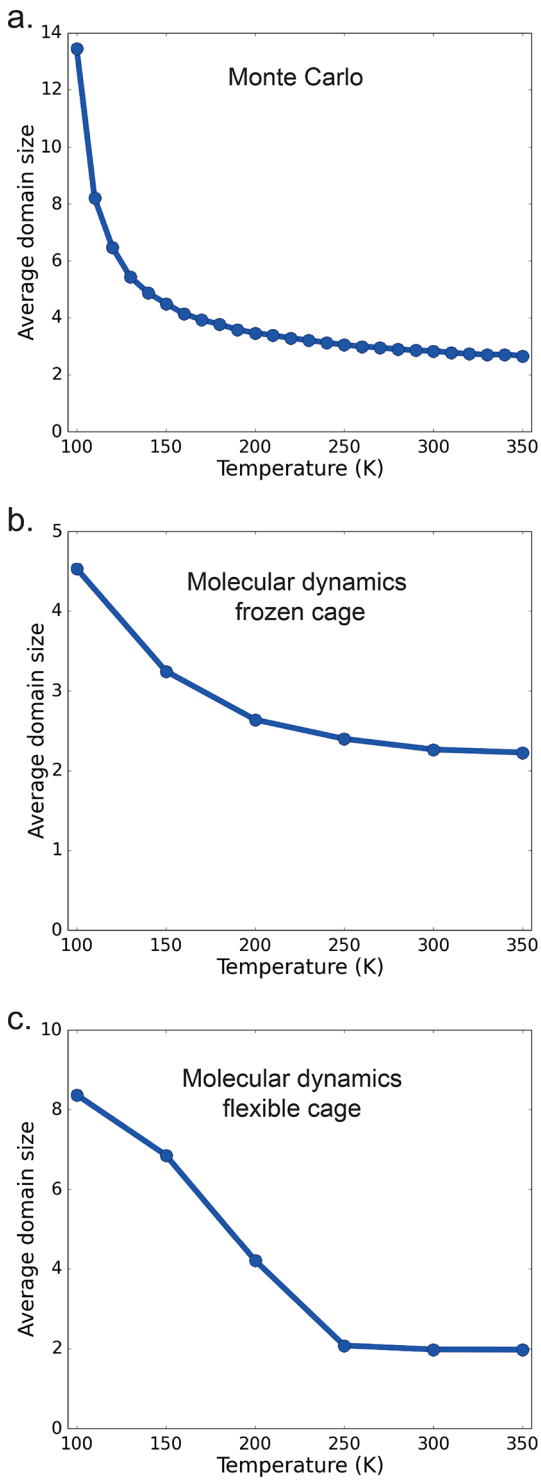

Figure 2. Average domain size vs temperature for methylammonium dipoles simulated with (a) Monte Carlo only considering dipole−dipole interaction, (b) molecular dynamics with frozen lead iodide cage, and (c) molecular dynamics with flexible lead iodide cage.

DOI: 10.1021/acs.jpcc.9b02736
J. Phys. Chem. C 2019, 123, 14652−14661

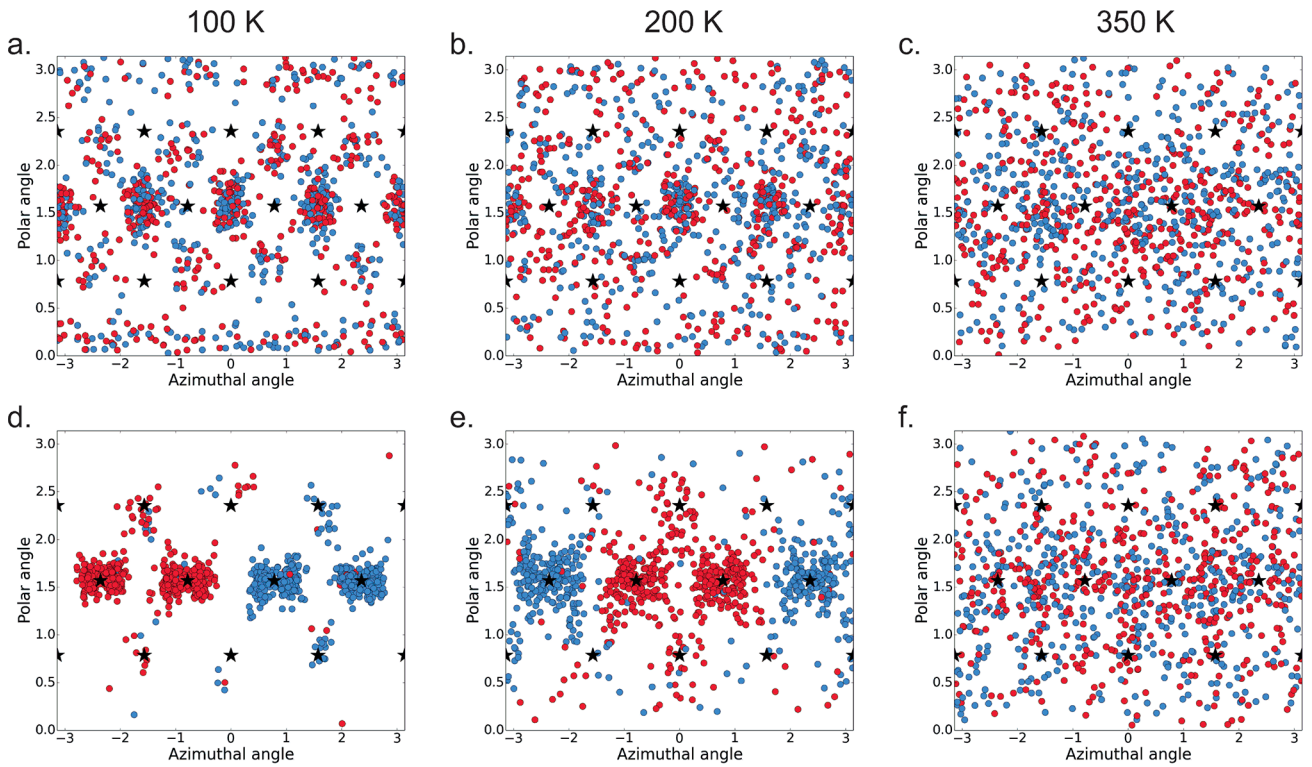

Figure 3. Orientations of all methylammonium dipoles in a single molecular dynamics system given in their polar and azimuthal angle: (a−c) frozen cage at 100, 200, and 350 K and (d−f) flexible cage at 100, 200, and 350 K. The stars in the figures represent the orientations where the dipole is oriented directly toward an iodine.

This can be interpreted as a phase transition of sorts; at the temperature where k_BT becomes comparable to the dipole−dipole interaction energy the ions align together due to their interactions with one another.

Figure 2b shows the same domain detection analysis on the MA ions in the MD simulations with a frozen cage. By comparing this to the simulations that only consider dipole−dipole interaction, we gain insight into the relative importance of the dipole−dipole interactions when specific interactions with the Pb−I cage are also taken into account. The frozen cage MD simulations show a similar trend in domain growth as the MC simulations. The increase in average domain size is, however, a lot smaller in this temperature range. This shows that with a surrounding cage the MA ions are still affected by interaction with one another at low temperatures. However, the effect is less pronounced because specific interactions between the MA and the cage also play a role here.

To complete the comparison, we show the average size of domains of MA ions in the flexible cage MD simulations as a function of temperature in Figure 2c. These systems show a different behavior compared to the other two. First of all, the increase of the average domain size occurs at higher temperatures. Between 250 and 200 K there is an abrupt increase in the average domain size, whereas for the other systems a notable increase was not seen until at roughly 150 K. Furthermore, the nature of the increase is different compared to the MC system. In the case of the flexible MD simulations we do not observe a gradual exponential increase but instead an abrupt linear increase that seems to start saturating at the lowest simulated temperature. These differences are comparable to the difference we saw between rotation-autocorrelation plots for the flexible- and frozen-cage MD simulations. In the autocorrelation decays, an abrupt step was seen between 200 and 250 K for flexible Pb−I cages, resulting in less reorientation of the methylammonium ions at the lower temperature. This was not seen in the case of the frozen cage.

Effect of Specific Interactions between MA and Cage. Having investigated the effect of cage movement and dipole−dipole interaction, the final step is to understand the role of specific interactions between the lead iodide cage and MA ion. To achieve this, we have analyzed the MD simulations above in more detail, paying specific attention to the directions of the MA ions in a single system with respect to the lead iodide cage. This is done by plotting scatter plots with all MA directions obtained from a single simulation snapshot. Each point is then the direction of a single ion represented in its azimuthal and polar angles. We do this to observe whether certain ion directions within the cage become more prominent than others as the temperature is changed. Two different colors are used for the points to evaluate whether there is a difference between the neighboring layers in the system. Odd number layers are portrayed by blue points, and even number layers are indicated in red. In these figures, the stars represent the directions that correspond to an MA ion pointing directly toward an iodine molecule in a cubic cage. These plots are shown in Figure 3 for both MD simulations with flexible and frozen cage at 100, 200, and 350 K. Similar figures were made for the other simulated temperatures and for the dipole−dipole MC simulations; these figures can be found in the Supporting Information. For the MC simulations there is no preferred MA orientation visible at any temperature. This is not surprising as there is no cage to affect the orientation of the MA ions. So even though the MA ions start to align favorably with one another at low temperatures and form domains, they do not necessarily

DOI: 10.1021/acs.jpcc.9b02736
J. Phys. Chem. C 2019, 123, 14652−14661

align all in the same direction. A similar trend has been seen before in a two-dimensional Monte Carlo study, where very low temperatures where needed to align all the MA ions in a certain way.[14]

Figures 3a–c show the directional ordering for the frozen-cage MD simulations at 100, 200, and 350 K. At 350 K the alignment of the ions is random over the spherical surface; the reason for higher density at central polar angles is that this is a spherical surface projected on a rectangular graph. As the temperature is lowered to 200 K a structure emerges, with some orientations becoming more prominent than others. At 100 K this is even stronger. Surprisingly, the most common orientations are not directed toward iodines, as one would expect if the MA forms hydrogen bonds with the iodine. Furthermore, no difference is seen between different layers in these simulations.

Figures 3d–f represent the flexible cage MD simulations at 100, 200, and 350 K. Again the alignment is random at 350 K, and a more organized structure is formed when the temperature is lowered. In this case, however, the effect is much more pronounced with the ions aligning all in the same plane at the lowest temperature and each adjacent layer aligning antiparallel to its neighbor. Within each layer there are two main orientations, both where one would assume a hydrogen bond is formed. This is in agreement with previous *ab initio* and model potential molecular dynamics studies were same alignment was seen and attributed to the low temperature orthorhombic phase.[12,14]

To get some insight into the dynamics of the specific interaction, we have analyzed the time scale on which the hydrogen bonds are broken. In this case we consider a hydrogen bond to occur when the distance between a hydrogen and an iodine is <3 Å. These hydrogen bond lifetimes are shown in Figure 4b as a function of temperature. It is clear from this figure that the time that hydrogen bonds exist in MA is very short, except at 100 K where a lifetime over 10 ps is obtained. This is consistent with the large degree of rotational freedom discussed above; even if the general direction is frozen, the wobbling motion still allows a considerable freedom for the MA to move around.

Formamidinium Lead Iodide (FAPI). In a similar way as for MAPI, full molecular dynamics simulations were performed for FAPI. A trajectory of the FA cations is obtained over 100 ps after equilibration of the system. The rotation-autocorrelation function averaged over the 1000 FA dipoles is shown as a function of time in Figure 5a. The simulations were performed at temperatures starting from 100 to 350 K in steps of 50 K. The trends observed for FAPI exhibit substantial differences compared to those presented above for MAPI. The decay of the autocorrelation function shows a more gradual variation with temperature, indicating that in the same temperature range no strong phase transitions are observed. At 300 and 350 K the rotation time for FA is larger than for MA, as can be seen in Table 2. This contradicts some of the previous experimental and theoretical work where the rotation time for FA was of similar magnitude or smaller than for MA.[23,29,30] However, the rotation time at 350 K is already a lot faster, implying that these differences could be a result of shortcomings in the force field, as already mentioned above. To unravel the different contributions to the observed rotational dynamics of FA in FAPI, we have performed the same model calculations as for MAPI, as described below.

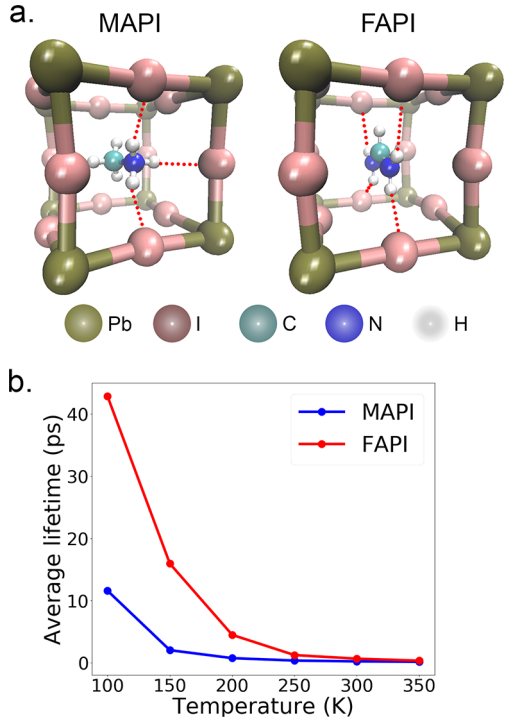

Figure 4. (a) Hydrogen bonds formed in MAPI and FAPI between the hydrogens of amine group and iodide atoms of the cage. (b) Hydrogen bond lifetime in picoseconds averaged for the hydrogen bonds formed for MAPI and FAPI.

Effect of Cage Deformation. The rotation-autocorrelation function for the motion of FA in a fixed Pb–I cage structure is shown as a function of time in Figure 5b. This figure and the rotation times in Table 2 show that also for the fixed cage a gradual decrease in the rotation times is observed with increasing temperature. No abrupt changes due to phase transitions are formed. Comparison with Figure 5a shows that cage deformation leads to an overall slower dynamics, as was also the case for MAPI; however, the effect is not as pronounced as for MAPI. Nevertheless, these simulations show that the deformation of the Pb–I cage also plays a significant role in the rotation dynamics in FAPI.

Effect of Dipole–Dipole Interactions. The effect of the dipole–dipole interactions on the FA alignment in FAPI was again evaluated by comparing the size of the ordered domains formed at various temperatures for the three different simulation types, that is, MC simulations considering only dipole–dipole interactions, molecular dynamics with a frozen Pb–I cages, and fully flexible molecular dynamics simulations. The average domain size for these three cases is plotted as a function of temperature in Figure 6.

In the case of the MC simulations where only dipole–dipole interactions are considered the domain size is unaffected by the temperature in the considered temperature range, implying that the dipole–dipole interactions are not large enough to affect the ion alignments. This is due to the much smaller dipole moment of the FA ion compared to the MA ion. This results in dipole–dipole interactions that are much smaller than k_BT at the temperatures considered, and hence the thermal energy is high enough to prevent the formation of domains. This implies that the phase transition in FAPI should not be affected by the dipole–dipole interaction of FA ions.

DOI: 10.1021/acs.jpcc.9b02736
J. Phys. Chem. C 2019, 123, 14652–14661

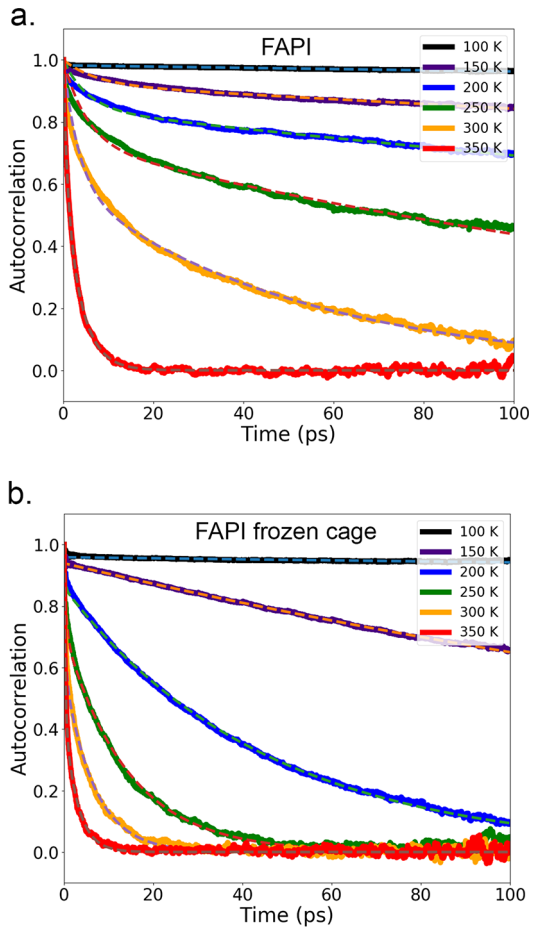

Figure 5. (a) Rotation autocorrelation of the dipole direction averaged over 1000 dipoles for FA cations in a flexible lead iodide cage at temperatures ranging from 100 to 350 K. (b) Rotation autocorrelation of the dipole direction averaged over 1000 dipoles for FA cations in a frozen lead iodide cage at temperatures ranging from 100 to 350 K.

Table 2. Rotation-Autocorrelation Decay Time Constants for FA (in picoseconds) Obtained after Fitting the Decay Curves in Figure 5 by Using Eq 3[a]

	flexible cage		frozen cage	
T (K)	τ_1 (ps) (A_1)	τ_2 (ps) (A_2)	τ_1 (ps) (A_1)	τ_2 (ps) (A_2)
100	0.05 (0.02)	>1000 (0.98)	0.05 (0.04)	>1000 (0.96)
150	7.14 (0.08)	>1000 (0.92)	0.04 (0.06)	271.73 (0.94)
200	5.24 (0.16)	510.27 (0.84)	0.23 (0.14)	45.12 (0.86)
250	5.21 (0.27)	195.40 (0.73)	0.45 (0.28)	14.21 (0.72)
300	3.41 (0.40)	52.63 (0.60)	0.31 (0.41)	6.60 (0.59)
350	0.77 (0.34)	3.62 (0.66)	0.27 (0.54)	2.89 (0.46)

[a] τ_1 corresponds to the faster decay time, whereas τ_2 corresponds to the slower decay time constant.

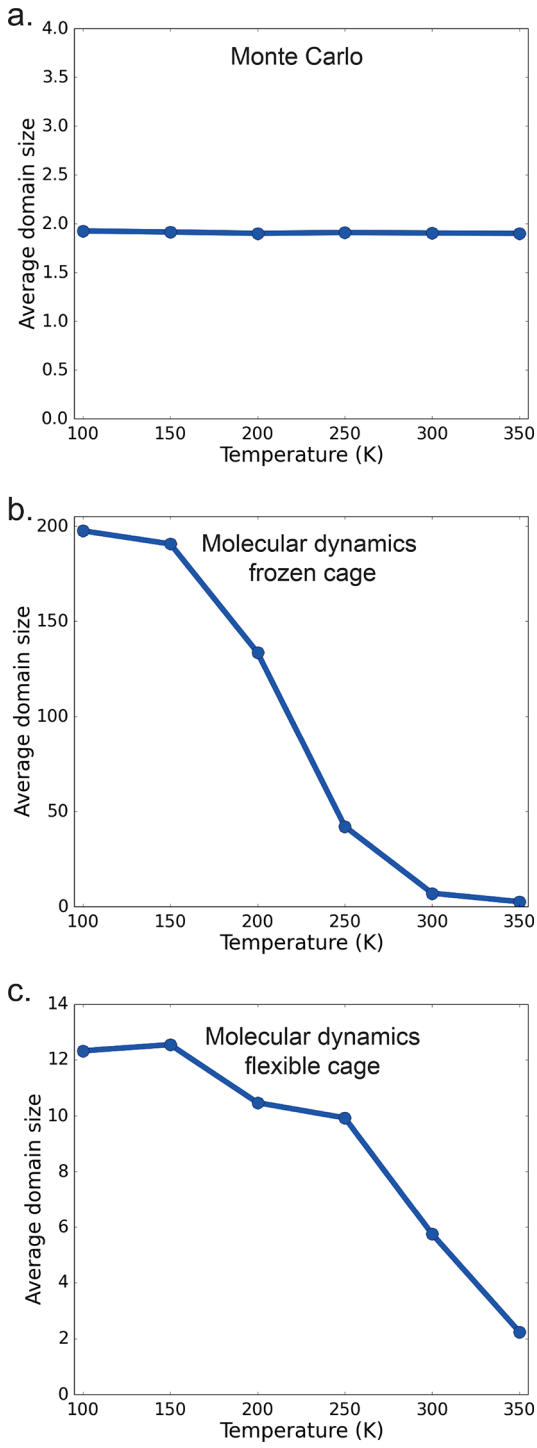

Figure 6. Average domain size vs temperature for formamidinium dipoles simulated with (a) Monte Carlo only considering dipole−dipole interaction, (b) molecular dynamics with frozen lead iodide cage, and (c) molecular dynamics with flexible lead iodide cage.

Interestingly, we observe an increase in domain size with lower temperatures for both molecular dynamics systems. This results in large domains at low temperatures, especially in the case of the frozen cage. As we have excluded the possibility of a dipole−dipole effect, it is likely that this happens due to some interaction between the ion and the cage that causes certain ion alignments to be more prominent than others.

Effect of Specific Interactions between FA and Cage. To further investigate to what extent the FA ions interact with the lead iodide cage, we again look at scatter plots with all dipole directions of the FA ions in a single system, for molecular dynamics simulations with both the frozen and flexible cage. The obtained results at 100, 200, and 350 K can be observed in Figure 7.

For both simulations we can already see that the ion alignment is not completely random at high temperatures as there is higher density at certain angles. In both cases these are

DOI: 10.1021/acs.jpcc.9b02736
J. Phys. Chem. C 2019, 123, 14652−14661

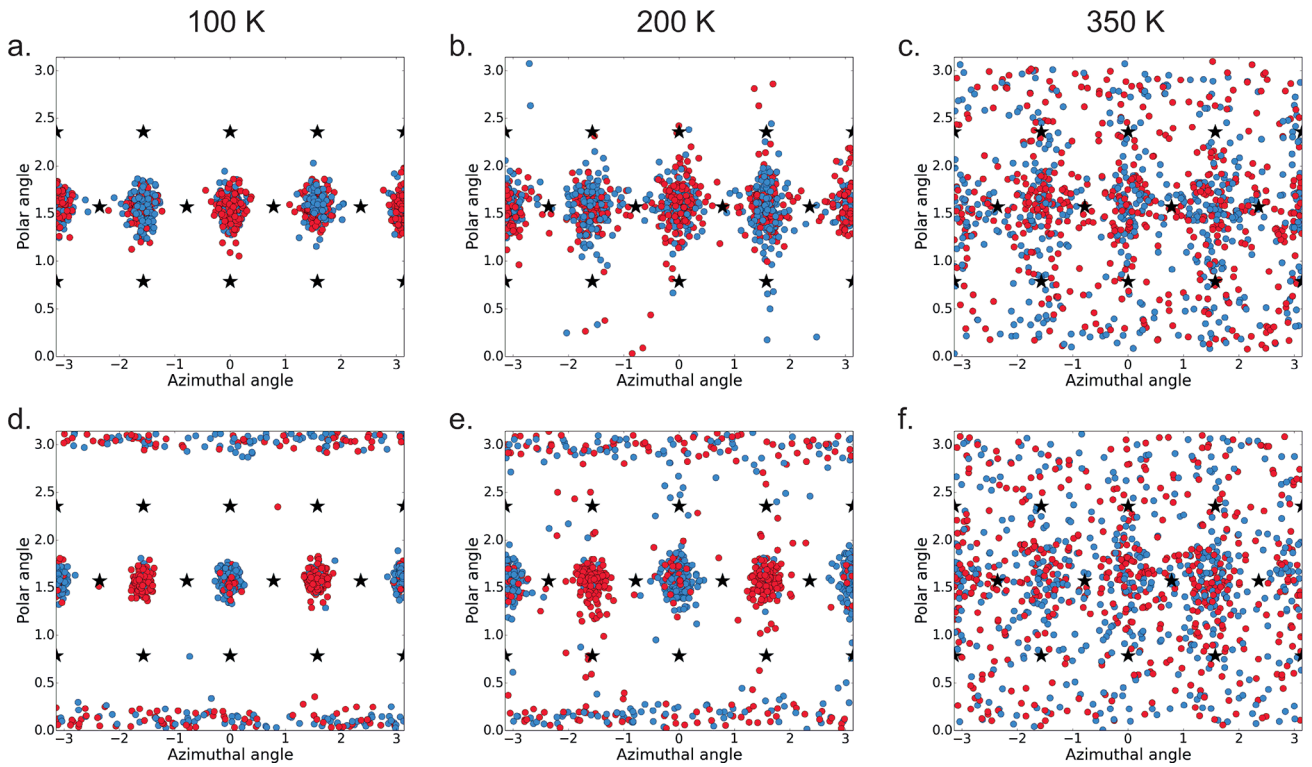

Figure 7. Orientations of all formamidinium dipoles in a single molecular dynamics system given in their polar and azimuthal angle: (a–c) frozen cage at 100, 200, and 350 K and (d–f) flexible cage at 100, 200, and 350 K. The stars in the figures represent the orientations where the dipole is oriented directly toward an iodine.

angles that lead to the dipole of the FA ion pointing in between two iodines. This can be explained through hydrogen bonding between iodine and the hydrogens on the nitrogen molecules. If the dipole points between two iodines, the nitrogens can point toward the iodines, allowing the hydrogen bonds to form. As the temperature is lowered, these alignments become more prominent in both cases.

This high degree of order in the FA orientation at low temperatures explains why large domains were observed for these systems above. If the ion alignments are restricted to only few possible orientations, large domains will be obtained even though the dipole–dipole interactions do not play any role in the alignment. One major difference is visible between the low-temperature simulations for the frozen and flexible cage. For the flexible cage the FA ions align both in the azimuthal plane and perpendicular to it. In the frozen cage simulations the ions however only align in the azimuthal plane.

To gain insight into the time scale of the specific interaction, we have again analyzed the hydrogen bond lifetimes as shown in Figure 4b. The lifetimes observed for FAPI at low temperature are considerably longer than for MAPI. One may interpret this as an indication of stronger hydrogen bonds; however, the lifetime is affected by all the interactions in the system, including steric hindrance that hampers the rotational motion of FA in the Pb–I cage and the effect due to cage deformation.

CONCLUSIONS

It is clear from the simulations presented above that the phase behavior and the rotational dynamics of the organic cation are intricately linked for both MAPI and FAPI. For MAPI a very clear phase transition is observed at which the MA cation becomes immobilized, and at the same time the Pb–I lattice deforms. The phase transition is accompanied by the formation of domains in which the MA dipoles arrange in an ordered, energetically favorable structure. This domain formation is already observed if only the dipole–dipole interactions are taken into account, but the effect becomes much stronger if the cations are embedded in the Pb–I lattice, especially when the lattice is allowed to deform in reaction to the alignment. This points to a mechanism where phase transitions are induced by mutual alignment of the dipoles, by both interactions with neighboring dipole and specific interactions between the MA cations and the Pb–I lattice. This happens in a concerted way with the deformation of the Pb–I lattice, which strengthens this effect and makes the transition from freely rotating dipoles to ordered domains with fixed dipole directions more abrupt at a certain temperature. This importance of the cage flexibility on the MA dynamics is in good agreement with previous experimental and theoretical work.[37,38]

For FAPI a very similar picture emerges; however, in this case the dipole–dipole interactions in the nondipolar FA cation are negligible. Simulations of the dipole dynamics in fixed, cubic Pb–I cage structures show that specific interactions between FA and the Pb and I ions, and between the quadrupolar FA ions, still lead to the formation of ordered domains, even if the Pb–I lattice is not allowed to deform. In the fully flexible MD simulations where full relaxation of the lattice is possible, this effect is strengthened, and domain formation is more abrupt at a certain temperature. As discussed above, the formation of hydrogen-bond-like conformations plays an important role in FAPI, which, combined with increased steric interactions, leads to slower rotation dynamics of FA in FAPI.

DOI: 10.1021/acs.jpcc.9b02736
J. Phys. Chem. C 2019, 123, 14652–14661

We conclude that the phase transitions that occur in hybrid halide perovskites are caused by a complex interplay between dipole−dipole interactions, specific electrostatic and steric interactions between the organic cations and the metal halide lattice, and relaxation of the metal halide cage structure. This leads to large organized domains of organic cations, which can have important consequences for the electronic structures of these materials.

■ ASSOCIATED CONTENT

Supporting Information

The Supporting Information is available free of charge on the ACS Publications website at DOI: 10.1021/acs.jpcc.9b02736.

All the parameters used for molecular dynamics force field (Tables S1−S6); model validation calculations for both MAPI and FAPI (Figure S1); directional scatter plots for Monte Carlo and both versions of molecular dynamics simulations at all simulated temperatures for MAPI (Figure S2) and FAPI (Figure S3) (PDF)

■ AUTHOR INFORMATION

Corresponding Author

*E-mail: f.c.grozema@tudelft.nl.

ORCID

Jörg Meyer: 0000-0003-0146-730X

Ferdinand C. Grozema: 0000-0002-4375-799X

Author Contributions

S.M. and M.B.F. contributed equally to this work.

Notes

The authors declare no competing financial interest.

■ ACKNOWLEDGMENTS

This work is part of an Industrial Partnership Programme of the Foundation for Fundamental Research on Matter (FOM), which is part of The Netherlands Organisation for Scientific Research (NWO). The research leading to these results in the Delft University of Technology has received funding from the European Research Council Horizon 2020 ERC Grant Agreement No. 648433. J.M. acknowledges financial support from The Netherlands Organisation for Scientific Research (NWO) under Vidi Grant No. 723.014.009.

■ REFERENCES

(1) Brauer, J. C.; Lee, Y. H.; Nazeeruddin, M. K.; Banerji, N. Charge Transfer Dynamics from Organometal Halide Perovskite to Polymeric Hole Transport Materials in Hybrid Solar Cells. *J. Phys. Chem. Lett.* **2015**, *6*, 3675−3681.

(2) NREL Best Research Cell Efficiency, howpublished = https://www.nrel.gov/pv/assets/images/efficiency-chart.png, note = Accessed: 2018-05-14.

(3) Shin, S. S.; Yeom, E. J.; Yang, W. S.; Hur, S.; Kim, M. G.; Im, J.; Seo, J.; Noh, J. H.; Seok, S. I. Colloidally Prepared La-Doped BaSnO3 Electrodes for Efficient, Photostable Perovskite Solar Cells. *Science* **2017**, *356*, 167−171.

(4) Umari, P.; Mosconi, E.; De Angelis, F. Infrared Dielectric Screening Determines the Low Exciton Binding Energy of Metal-Halide Perovskites. *J. Phys. Chem. Lett.* **2018**, *9*, 620−627.

(5) Leguy, A. M. A.; Frost, J. M.; McMahon, A. P.; Sakai, V. G.; Kockelmann, W.; Law, C.; Li, X.; Foglia, F.; Walsh, A.; O'Regan, B. C.; et al. The Dynamics of Methylammonium Ions in Hybrid Organic-Inorganic Perovskite Solar Cells. *Nat. Commun.* **2015**, *6*, 7124.

(6) Wu, X.; Trinh, M. T.; Niesner, D.; Zhu, H.; Norman, Z.; Owen, J. S.; Yaffe, O.; Kudisch, B. J.; Zhu, X.-Y. Trap States in Lead Iodide Perovskites. *J. Am. Chem. Soc.* **2015**, *137*, 2089−2096.

(7) Weller, M. T.; Weber, O. J.; Henry, P. F.; Di Pumpo, A. M.; Hansen, T. C. Complete Structure and Cation Orientation in the Perovskite Photovoltaic Methylammonium Lead Iodide Between 100 and 352 K. *Chem. Commun.* **2015**, *51*, 4180−4183.

(8) Gélvez-Rueda, M. C.; Cao, D. H.; Patwardhan, S.; Renaud, N.; Stoumpos, C. C.; Schatz, G. C.; Hupp, J. T.; Farha, O. K.; Savenije, T. J.; Kanatzidis, M. G.; et al. Effect of Cation Rotation on Charge Dynamics in Hybrid Lead Halide Perovskites. *J. Phys. Chem. C* **2016**, *120*, 16577−16585.

(9) Bernard, G. M.; Wasylishen, R. E.; Ratcliffe, C. I.; Terskikh, V.; Wu, Q.; Buriak, J. M.; Hauger, T. Methylammonium Cation Dynamics in Methylammonium Lead Halide Perovskites: A Solid-State NMR Perspective. *J. Phys. Chem. A* **2018**, *122*, 1560−1573.

(10) Whitfield, P. S.; Herron, N.; Guise, W. E.; Page, K.; Cheng, Y. Q.; Milas, I.; Crawford, M. K. Structures, Phase Transitions and Tricritical Behavior of the Hybrid Perovskite Methyl Ammonium Lead Iodide. *Sci. Rep.* **2016**, *6*, 35685.

(11) Poglitsch, A.; Weber, D. Dynamic Disorder in Methylammoniumtrihalogenoplumbates (II) Observed by Millimeter-Wave Spectroscopy. *J. Chem. Phys.* **1987**, *87*, 6373−6378.

(12) Mattoni, A.; Filippetti, A.; Saba, M. I.; Delugas, P. Methylammonium Rotational Dynamics in Lead Halide Perovskite by Classical Molecular Dynamics: The Role of Temperature. *J. Phys. Chem. C* **2015**, *119*, 17421−17428.

(13) Guo, Y.; Yaffe, O.; Paley, D. W.; Beecher, A. N.; Hull, T. D.; Szpak, G.; Owen, J. S.; Brus, L. E.; Pimenta, M. A. Interplay Between Organic Cations and Inorganic Framework and Incommensurability in Hybrid Lead-Halide Perovskite $CH_3NH_3PbBr_3$. *Phys. Rev. Mater.* **2017**, *1*, 42401.

(14) Frost, J. M.; Butler, K. T.; Walsh, A. Molecular Ferroelectric Contributions to Anomalous Hysteresis in Hybrid Perovskite Solar Cells. *APL Mater.* **2014**, *2*, 081506.

(15) Li, J.; Rinke, P. Atomic Structure of Metal-Halide Perovskites from First Principles: The Chicken-and-Egg Paradox of the Organic-Inorganic Interaction. *Phys. Rev. B: Condens. Matter Mater. Phys.* **2016**, *94*, 45201.

(16) Bokdam, M.; Lahnsteiner, J.; Ramberger, B.; Schäfer, T.; Kresse, G. Assessing Density Functionals Using Many Body Theory for Hybrid Perovskites. *Phys. Rev. Lett.* **2017**, *119*, 145501.

(17) Lahnsteiner, J.; Kresse, G.; Kumar, A.; Sarma, D. D.; Franchini, C.; Bokdam, M. Room-Temperature Dynamic Correlation Between Methylammonium Molecules in Lead-Iodine Based Perovskites: An ab initio Molecular Dynamics Perspective. *Phys. Rev. B: Condens. Matter Mater. Phys.* **2016**, *94*, 214114.

(18) Carignano, M. A.; Kachmar, A.; Hutter, J. Thermal Effects on CH3NH3PbI3 Perovskite from Ab Initio Molecular Dynamics Simulations. *J. Phys. Chem. C* **2015**, *119*, 8991−8997.

(19) Govinda, S.; Kore, B. P.; Bokdam, M.; Mahale, P.; Kumar, A.; Pal, S.; Bhattacharyya, B.; Lahnsteiner, J.; Kresse, G.; Franchini, C.; et al. Behavior of Methylammonium Dipoles in MAPbX3 (X = Br and I). *J. Phys. Chem. Lett.* **2017**, *8*, 4113−4121.

(20) Selig, O.; Sadhanala, A.; Müller, C.; Lovrincic, R.; Chen, Z.; Rezus, Y. L. A.; Frost, J. M.; Jansen, T. L. C.; Bakulin, A. A. Organic Cation Rotation and Immobilization in Pure and Mixed Methylammonium Lead-Halide Perovskites. *J. Am. Chem. Soc.* **2017**, *139*, 4068−4074.

(21) Handley, C. M.; Freeman, C. L. A New Potential for Methylammonium Lead Iodide. *Phys. Chem. Chem. Phys.* **2017**, *19*, 2313−2321.

(22) Weller, M. T.; Weber, O. J.; Frost, J. M.; Walsh, A. Cubic Perovskite Structure of Black Formamidinium Lead Iodide, α-[HC(NH2)2]PbI3, at 298 K. *J. Phys. Chem. Lett.* **2015**, *6*, 3209−3212.

(23) Fabini, D. H.; Siaw, T. A.; Stoumpos, C. C.; Laurita, G.; Olds, D.; Page, K.; Hu, J. G.; Kanatzidis, M. G.; Han, S.; Seshadri, R.

DOI: 10.1021/acs.jpcc.9b02736
J. Phys. Chem. C 2019, 123, 14652−14661

Universal Dynamics of Molecular Reorientation in Hybrid Lead Iodide Perovskites. *J. Am. Chem. Soc.* **2017**, *139*, 16875−16884.
(24) Carignano, M. A.; Saeed, Y.; Aravindh, S. A.; Roqan, I. S.; Even, J.; Katan, C. A Close Examination of the Structure and Dynamics of HC(NH2)2PbI3 by MD Simulations and Group Theory. *Phys. Chem. Chem. Phys.* **2016**, *18*, 27109−27118.
(25) Weber, O. J.; Ghosh, D.; Gaines, S.; Henry, P. F.; Walker, A. B.; Islam, M. S.; Weller, M. T. Phase Behavior and Polymorphism of Formamidinium Lead Iodide. *Chem. Mater.* **2018**, *30*, 3768−3778.
(26) Gallop, N. P.; Selig, O.; Giubertoni, G.; Bakker, H. J.; Rezus, Y. L. A.; Frost, J. M.; Jansen, T. L. C.; Lovrincic, R.; Bakulin, A. A. Rotational Cation Dynamics in Metal Halide Perovskites: Effect on Phonons and Material Properties. *J. Phys. Chem. Lett.* **2018**, *9*, 5987−5997.
(27) Bakulin, A. A.; Selig, O.; Bakker, H. J.; Rezus, Y. L.; Müller, C.; Glaser, T.; Lovrincic, R.; Sun, Z.; Chen, Z.; Walsh, A.; et al. Real-Time Observation of Organic Cation Reorientation in Methylammonium Lead Iodide Perovskites. *J. Phys. Chem. Lett.* **2015**, *6*, 3663−3669.
(28) Chen, T.; Foley, B. J.; Ipek, B.; Tyagi, M.; Copley, J. R. D.; Brown, C. M.; Choi, J. J.; Lee, S.-H. Rotational Dynamics of Organic Cations in the CH3NH3PbI3 Perovskite. *Phys. Chem. Chem. Phys.* **2015**, *17*, 31278−31286.
(29) Kubicki, D. J.; Prochowicz, D.; Hofstetter, A.; Péchy, P.; Zakeeruddin, S. M.; Grätzel, M.; Emsley, L. Cation Dynamics in Mixed-Cation (MA)x(FA)1-xPbI3 Hybrid Perovskites from Solid-State NMR. *J. Am. Chem. Soc.* **2017**, *139*, 10055−10061.
(30) Taylor, V. C. A.; Tiwari, D.; Duchi, M.; Donaldson, P. M.; Clark, I. P.; Fermin, D. J.; Oliver, T. A. A. Investigating the Role of the Organic Cation in Formamidinium Lead Iodide Perovskite Using Ultrafast Spectroscopy. *J. Phys. Chem. Lett.* **2018**, *9*, 895−901.
(31) Zoete, V.; Cuendet, M. A.; Grosdidier, A.; Michielin, O. SwissParam: A Fast Force Field Generation Tool for Small Organic Molecules. *J. Comput. Chem.* **2011**, *32*, 2359−2368.
(32) Vanommeslaeghe, K.; Hatcher, E.; Acharya, C.; Kundu, S.; Zhong, S.; Shim, J.; Darian, E.; Guvench, O.; Lopes, P.; Vorobyov, I.; et al. CHARMM General Force Field: A Force Field for Drug-Like Molecules Compatible with the CHARMM All-Atom Additive Biological Force Fields. *J. Comput. Chem.* **2010**, *31*, 671−690.
(33) Vanommeslaeghe, K.; MacKerell, A. D. Automation of the CHARMM General Force Field (CGenFF) I: Bond Perception and Atom Typing. *J. Chem. Inf. Model.* **2012**, *52*, 3144−3154.
(34) Vanommeslaeghe, K.; Raman, E. P.; MacKerell, A. D. Automation of the CHARMM General Force Field (CGenFF) II: Assignment of Bonded Parameters and Partial Atomic Charges. *J. Chem. Inf. Model.* **2012**, *52*, 3155−3168.
(35) Plimpton, S. Fast Parallel Algorithms for Short-Range Molecular Dynamics. *J. Comput. Phys.* **1995**, *117*, 1−19.
(36) Frost, J. M.; Walsh, A. What Is Moving in Hybrid Halide Perovskite Solar Cells? *Acc. Chem. Res.* **2016**, *49*, 528−535.
(37) Liao, W.-Q.; Zhang, Y.; Hu, C.-L.; Mao, J.-G.; Ye, H.-Y.; Li, P.-F.; Huang, S. D.; Xiong, R.-G. A Lead-Halide Perovskite Molecular Ferroelectric Semiconductor. *Nat. Commun.* **2015**, *6*, 7338.
(38) Zhang, Q.; Solanki, A.; Parida, K.; Giovanni, D.; Li, M.; Jansen, T. L. C.; Pshenichnikov, M. S.; Sum, T. C. Tunable Ferroelectricity in Ruddlesden-Popper Halide Perovskites. *ACS Appl. Mater. Interfaces* **2019**, *11*, 13523−13532.

DOI: 10.1021/acs.jpcc.9b02736
J. Phys. Chem. C 2019, 123, 14652−14661